

LASER BIOPHOTONICS

https://doi.org/10.1070/QEL17176

Experimental and theoretical description of the process of contact laser surgery with a titanium-doped optothermal fibre converter

A.V. Belikov, A.V. Skrypnik

Abstract. **In an *in vitro* experiment simulating a surgeon's actions in the process of contact laser surgery of soft biological tissue, the dependences of the temperature of a titanium-doped optothermal fibre converter (TOTFC) and the depths of coagulation and ablation of biological tissue on the average radiation power of a diode laser with a wavelength of 980 nm and on the speed of the converter movement along biological tissue are obtained. The structural, optical, and thermophysical models of TOTFC are discussed, as well as the thermophysical model of the interaction of a laser-heated converter with biological tissue, which takes into account the temperature dependences of the basic thermophysical parameters of the converter and biological tissue, as well as the contribution of the thickness h_{int} of the water vapour layer between the converter and biotissue. It is shown that the proposed model allows describing the result of contact laser surgery of soft biotissue with TOTFC adequately to the experiment.**

Keywords: *laser, converter, heating, biological tissue, surgery, water vapour, laser wound.*

1. Introduction

The development of new high-efficiency laser devices and methods to improve the quality of biological tissue processing and reduce the number of postoperative complications is one of the important tasks of modern laser physics, technology and medicine. In laser surgery, diode lasers are widely used for excision of soft tissues [1–4]. The radiation from most of these lasers lies in the wavelength range from 0.81 to 0.98 μm. The coefficient of light absorption by soft biological tissues in this spectral range does not exceed 1 cm^{-1} [4–6]. Such a small absorption leads to the fact that during the surgery of soft biological tissues, light penetrates deep enough into the biological tissue and is converted into heat with extremely low efficiency. As a result, biological tissues surrounding the affected area are seriously damaged; in some cases, the zone of thermal damage reaches several millimetres, which increases the healing time of the laser wound [7–10].

To increase the efficiency of the diode laser impact in contact surgery, optothermal fibre converters (OTFCs) are used, the purpose of which is to efficiently convert laser radiation into heat and to provide further destruction of biological tissue contacting with the converter heated to high temperatures [5, 11–15]. OTFCs are used for excision and coagulation of soft tissue during angioplasty [16–18], in dermatology [19–24], dentistry [25–27], neuroendoscopy [28–30], urology [31], etc.

Currently, a wide range of converters has been developed, differing primarily by light-absorbing material. For contact surgery using diode lasers, carbon-containing OTFCs are most often used [11, 14, 32–36]. As shown in Refs [15, 36], these converters are able to heat up to 1000 °C; however, a further increase in the temperature or average power of the laser radiation incident on the converter leads to their destruction and loss of their performance. The latter circumstance stimulates the search for alternative media for OTFCs. In [37], the fabrication technique, heating dynamics, and luminescence spectra of titanium-doped and erbium-doped OTFCs have been discussed. It has been shown that these converters are more resistant to laser heating than carbon-containing OTFCs, and the titanium-doped converter is capable of heating up to 2700 °C in air without destruction. In Ref. [38], life tests of carbon-containing and titanium-doped OTFC were performed. It was shown that the average lifetime of the Epic Pro C&Ti tip titanium-doped converter is 350 s, while the average lifetime of the Cork initiated tip and Pre-initiated tip carbon-containing converters is 10 and 60 s, respectively. In this regard, the titanium-doped OTFC (TOTFC) can be considered the most promising alternative to the widespread, but short-lived carbon-containing converter, and its optimisation is an urgent task. In Ref. [39], a comparative *in vitro* study of the effect of carbon-, titanium-, and erbium-doped converters on soft biological tissue in contact laser surgery using a diode laser was performed. It was demonstrated that the efficiency of excision of soft biological tissue, the thermal damage zone, and the temperature of the converters in contact with the soft biological tissue vary depending on the type of converter, the average laser radiation power, and the speed of the converter moving along the surface of the biological tissue. The maximum temperature of 1980 ± 154 °C, achieved by the converter during excision of the biological tissue, was recorded for TOTFC with an average laser power of 4.0 W and a speed of its movement along the biological tissue of 1 mm s^{-1}. The minimum temperature (540 ± 30 °C) at which tissue destruction occurs was also recorded for TOTFC with an average laser power of 1.0 W and a speed of its movement along the biological tissue of 6 mm s^{-1}. The maximum coagulation depth (0.72 ± 0.10 mm) was observed when using TOTFC with an average laser radiation power of 4.0 W and a speed of its movement along the biological tissue of 1 mm s^{-1}. The minimum coagulation depth (0.11 ± 0.02 mm) corresponded to the carbon-containing OTFC with an average radiation

A.V. Belikov ITMO University, Kronverksky prosp. 49, 197101 St. Petersburg, Russia; Pavlov First Saint Petersburg State Medical University, ul. L'va Tolstogo 6-8, 197022 St. Petersburg, Russia; e-mail: avbelikov@gmail.com;
A.V. Skrypnik ITMO University, Kronverksky prosp. 49, 197101 St. Petersburg, Russia

Received 31 October 2019; revision received 9 January 2020
Kvantovaya Elektronika **50** (2) 95–103 (2020)
Translated by V.L. Derbov

power of 0.3 W and a movement speed of 3 mm s^{-1}. The maximum excision efficiency (0.57 mm^3 W^{-1}) was observed for an erbium-doped OTFC at an average power of 1.0 W and a speed of 1 mm s^{-1}, and the minimum (0.02 mm^3 W^{-1}) for a carbon-containing converter at an average power of 4.0 W and a speed of 6 mm s^{-1}.

Paper [40] describes in detail the structure of the TOTFC used in contact laser surgery for excision and coagulation of soft biological tissues. Structural, optical, and thermophysical models of such a converter are proposed. The optical and thermophysical calculations performed within the framework of these models made it possible to estimate the fraction of the laser energy absorbed by the converter and the dynamics of its laser-induced heating in air. The results obtained are compared with experimental data on the heating of a TOTFC in air by radiation from a diode laser with a wavelength of 980 nm. The influence of the temperature dependences of density, specific heat, thermal conductivity, converter blackness, and converter–air and fibre–air heat transfer coefficient on the dynamics of laser heating of TOTFC is discussed. It is shown that the temperature dependence of the specific heat and the degree of blackness of the converter make the major contribution to the simulation results.

Unfortunately, to date, the theory that could allow describing the interaction of laser-heated OTFC with biological tissue is practically absent. In this regard, it is urgent to develop an adequate model that takes into account the characteristics of the interaction of TOTFC with a soft biological tissue and allows theoretical evaluation of the temperatures reached in the treatment zone and their comparison with the threshold values at which coagulation and carbonisation of soft biological tissue occur.

The objectives of this work are an experimental study of the effect of the average radiation power of a diode laser with a wavelength of 980 nm and the velocity of a titanium-doped OTFC moving along the surface of a soft biological tissue on the converter temperature, the depth of the tissue coagulation and ablation, as well as the search for parameters and the development of a model that adequately describes the interaction of TOTFC with a soft biological tissue.

2. Structure and properties of a titanium-doped optothermal fibre converter

The process of fabricating a TOTFC is described in detail in Ref. [37]. The structural, optical, and thermophysical models of this converter are presented in Ref. [40]. TOTFC has a nearly spherical shape and is located on the distal end of a silica optical fibre (Fig. 1a). The distal end of the fibre penetrates deep into the converter. The fibre diameter inside the converter is 400 ± 10 μm. TOTFC is slightly elongated in the direction perpendicular to the fibre axis, its size being 700–800 μm. TOTFC has a strong mechanical bond with the fibre. The colour of TOTFC is mostly white with blue fragments. The blue colour indicates the presence of Ti_2O_3 in the composition of this converter, and the white colour indicates TiO_2 [41,42]. When the image is enlarged, microstructural elements become visible in the TOTFC, namely, scattering centres with a diameter of 1.2 ± 0.2 μm, almost uniformly distributed in its volume and separated by 1.6 ± 0.4 μm from each other. X-ray diffraction analysis shows that these scattering centres are titanium oxide, and the space between them is filled with silicon oxide.

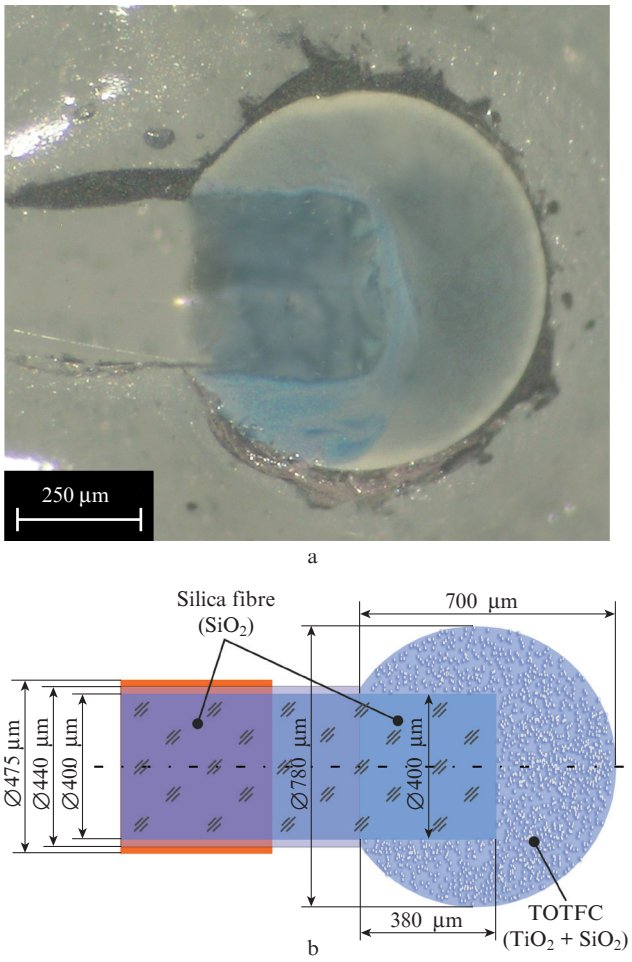

Figure 1. (a) Optical image of the TOTFC section and (b) its structural model [40].

The structural model of TOTFC is a spherical element with a diameter of D = 780 μm, deformed along the fibre axis by the size of a spherical segment with a height of h = 80 μm. A fragment of the light-guiding core of a cylindrical optical waveguide having a diameter of d = 400 μm is located inside the TOTFC at a depth of l = 380 μm (Fig. 1b). The internal microstructure of the TOTFC is modelled as a set of components uniformly distributed in the volume of the converter and representing densely packed cubes with the side a = 2.0 μm. In the middle of each cube there is a spherical titanium dioxide particle with the diameter d_{TiO_2} = 1.2 μm. The remaining free space of the cube is filled with silicon dioxide (silica). The volume fraction of silica k_{SiO_2} in TOTFC is 0.78; the volume fraction of titanium dioxide k_{TiO_2} is 0.22. The refractive index of the converter is 1.68, the absorption coefficient is 1.247 mm^{-1}, the scattering coefficient is 520.024 mm^{-1}, and the anisotropy factor is 0.38 [40].

TOTFC absorbs 83.5% of the laser radiation with a wavelength of 980 nm incident on it from the fibre side. In air, under the action of cw laser radiation with a wavelength of 980 nm and a power of 4.0 W, the TOTFC is heated to 2700 ± 50 °C, while it does not become destroyed and glows in the visible and IR spectral ranges [37,40].

The main thermophysical parameters of TOTFC [40] at room temperature are presented below.

Density ρ /kg m^{-3}	2653
Specific heat capacity c_p /J kg^{-1} K^{-1}	727
Thermal conductivity λ /W m^{-1} K^{-1}	3.2

The heat transfer coefficients at room temperature for fibre–air (α_{fa}) and converter–air (α_{ca}) pairs are 5.6 W m^{-2} K^{-1} [43]. The degree of blackness ε for TOTFC at room temperature is 0.906.

The temperature dependences of the above parameters in the temperature range of 20–3000 °C are discussed in detail in Ref. [40].

3. *In vitro* contact laser surgery of soft tissue with TOTFC

3.1. Experiment

In the process of *in vitro* contact surgery of soft biological tissue, TOTFC was in contact with the biological tissue and mechanically deformed its surface to a depth of about 200 μm. The converter moved along the surface of the biological tissue with a velocity V equal to 1, 3 or 6 mm s^{-1}. The average laser power P was 0.3, 1.0, or 4.0 W.

The muscle tissue of the chicken thigh, stored in a refrigerator at a temperature of 4 °C, was used as samples for *in vitro* studies. Before surgery, the biological tissue was kept at room temperature for 60 ± 1 min. In total, in the experiments, for each combination of the average power of laser radiation and the speed of TOTFC moving along the surface of the biological tissue, 10 cuts were performed on one sample of the biological tissue. The number 9 of biological tissue samples corresponded to the number of combinations.

In the study we used a diode-based laser system with a wavelength radiation of 980 ± 10 nm (IPG Photonics, USA). Laser radiation was transmitted through a silica–silica optical fibre. The diameter of the guiding core of the optical fibre was 400 ± 5 μm, the total diameter of the fibre without a polymer coating was 440 ± 5 μm, and with a polymer coating it was 475 ± 10 μm. The average radiation power at the fibre output reached 4.0 W. The laser generated a sequence of pulses with a duration of 400 μs, following each other with a repetition rate of 2 kHz. A pause of 100 μs between the laser pulses was necessary for recording the residual (after the laser pulse) heating in the zone of interaction between the TOTFC and biological tissue with a large signal-to-noise ratio. The laser setup incorporated an IR sensor FD10D (Thorlabs, USA), which measured the intensity of thermal radiation resulting from heating the TOTFC with laser radiation. The minimum temperature that could be measured due to the limited spectral sensitivity of the IR sensor and the internal noise of the receiving path was 270 ± 10 °C. The temperature was measured every 30 ms, and its values were stored in a computer memory. The temperature measurement error did not exceed 5%.

In the experiment, the sequence of actions (steps) that the surgeon performs when excising soft biological tissue was imitated (Fig. 2). The temperature of the TOTFC was recorded almost throughout the entire experiment ('thermo ON', see Fig. 2).

Initially (step 1), the TOTFC was in air for 1.0 s in the immediate vicinity of biological tissue. Next (step 2), laser radiation ('laser ON') was supplied to the TOTFC for 1.5 s. Then (step 3), the TOTFC was in contact with the biological tissue, after which (step 4) it moved along the surface of the biological tissue for 10.0 s. Further, the TOTFC contact with the biological tissue was interrupted (step 5), and the converter was exposed to air in the immediate vicinity of the biological tissue for 1.5 s (step 6), after which the laser radiation was turned off (step 7, 'laser OFF') and the temperature measurement of the TOTFC was stopped (step 8, 'thermo OFF'.). On completion, the samples were photographed from above by a Nikon D80 digital camera (Nikon Corporation, Japan), and then were cut along the TOTFC displacement axis using Feather Microtome blades High Profile pfm (Feather Safety Razor Co., Japan) and stained with NBTC dye. The painted sections were also photographed. The resulting photographs were analysed using the programme AxioVision rel. 4.8.2

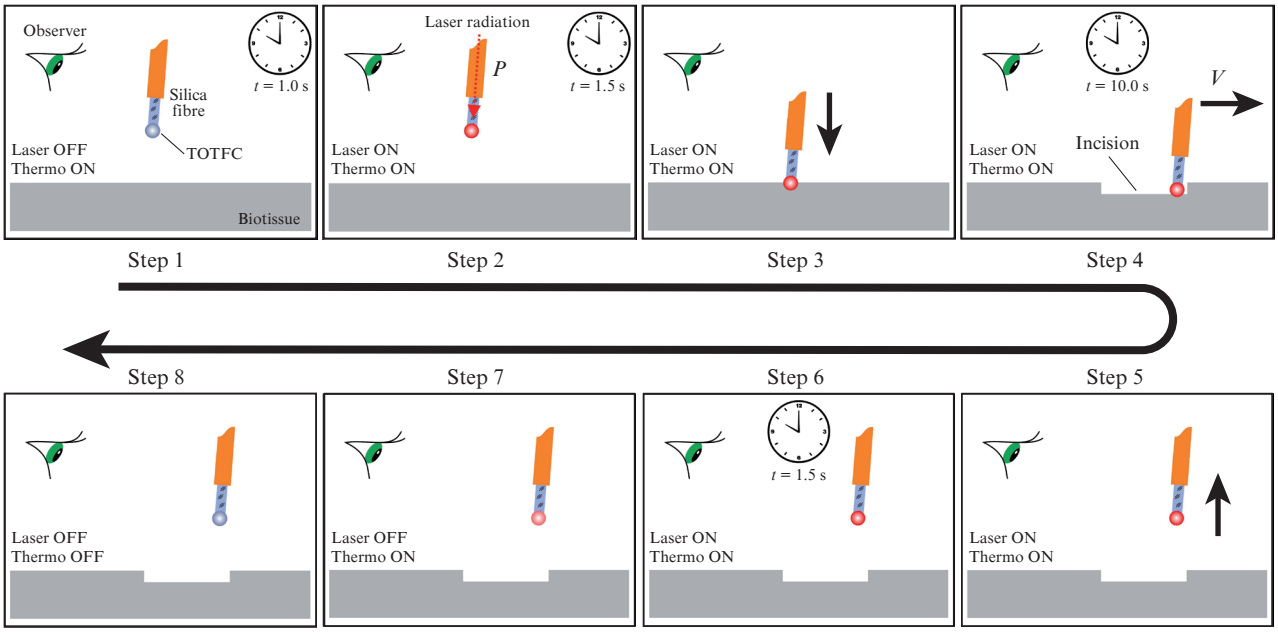

Figure 2. Sequence of actions (steps) imitating the actions of a surgeon in the process of laser excision of a soft biological tissue.

(Carl Zeiss GmbH, Germany) for determining the size of the zones of ablation and coagulation.

The complex of studies carried out allowed experimental determination of the dependences of the TOTFC temperature, the depths of ablation and coagulation of soft biological tissue during the interaction of the converter (step 4 in Fig. 2) on the average laser radiation power and the speed of the TOTFC movement (Figs 3 and 4).

At a constant speed of TOTFC movement, an increase in the average laser radiation power (Figs 3a and 4a) leads to an increase in the converter temperature, an increase in the depths of ablation and coagulation of biological tissue. At a constant average laser radiation power, an increase in the TOTFC moving speed (Figs 3b and 4b) leads to a decrease in the converter temperature and a decrease in the ablation and coagulation depths of the biological tissue.

An increase in the TOTFC temperature is accompanied by an increase in the depths of ablation and coagulation of biological tissue. The highest depths of biological tissue ablation and coagulation are 1030 ± 150 and 720 ± 100 μm, respectively, and are achieved at a TOTFC temperature of 1980 ± 154 °C. An increase in the TOTFC temperature with an increase in the average laser power is obviously associated with an increase in the average laser power absorbed by the converter. At the same time, the temperature of the TOTFC is also influenced by the speed of its movement through soft biological tissue. This may occur due to a change in the thickness of the layer of water vapour located between the TOTFC and the biological tissue, and a related change in the conditions of heat transfer from the TOTFC to its environment. For each converter moving speed its own optimal thickness of this layer is established. Such self-regulation occurs due to the equalisation of the speeds of movement of the evaporation front (from the converter to the biological tissue) and the movement of the converter. If the speed of movement of the evaporation front is greater than that of the converter, then the thickness of the layer of water vapour increases, and vice versa.

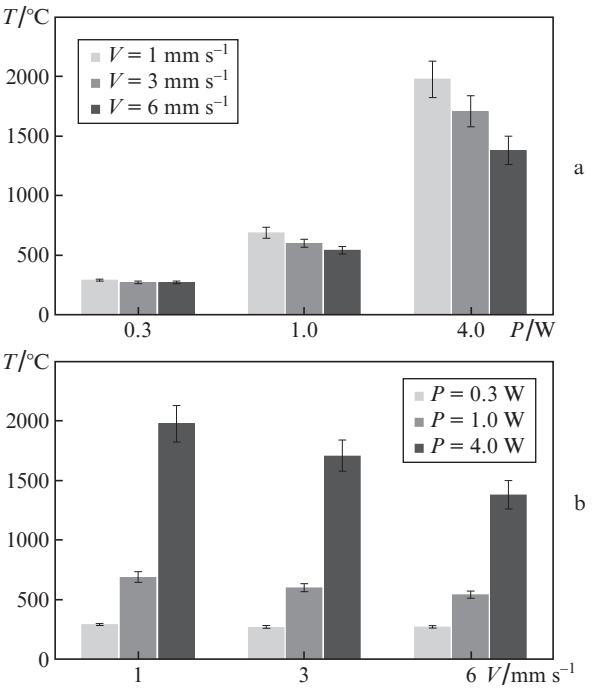

Figure 3. Dependences of the TOTFC temperature during contact surgery of soft biological tissue on (a) the average power of laser radiation and (b) its velocity of moving along the biological tissue surface.

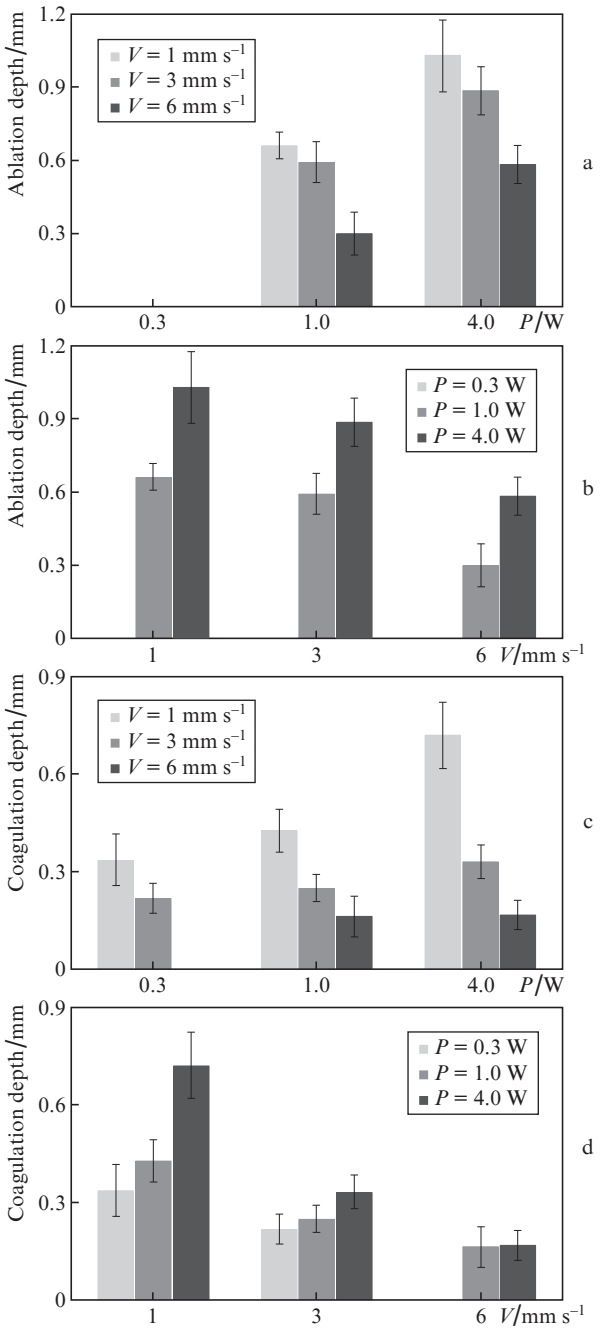

Figure 4. Dependences of the depths of ablation and coagulation of soft biological tissue during contact surgery using TOTFC on (a, c) the average laser radiation power and (b, d) its speed of movement along the surface of the biological tissue.

3.2. Theory

The laser heating of the TOTFC in air is described in detail in Ref. [40]. Unfortunately, in the literature the theory of the interaction of converters heated by laser radiation with biological tissue is virtually not discussed. In the present study, for the theoretical modelling of the TOTFC interaction with

a soft biological tissue, we used the scheme shown in Fig. 5. According to this scheme, laser radiation arrives at the TOTFC via an optical silica fibre with a diameter of 400 μm. The converter is buried in biological tissue (chicken thigh muscle tissue) to a depth of 200 μm. A layer of water vapour with the thickness h_{int} is located between the TOTFC and the biological tissue.

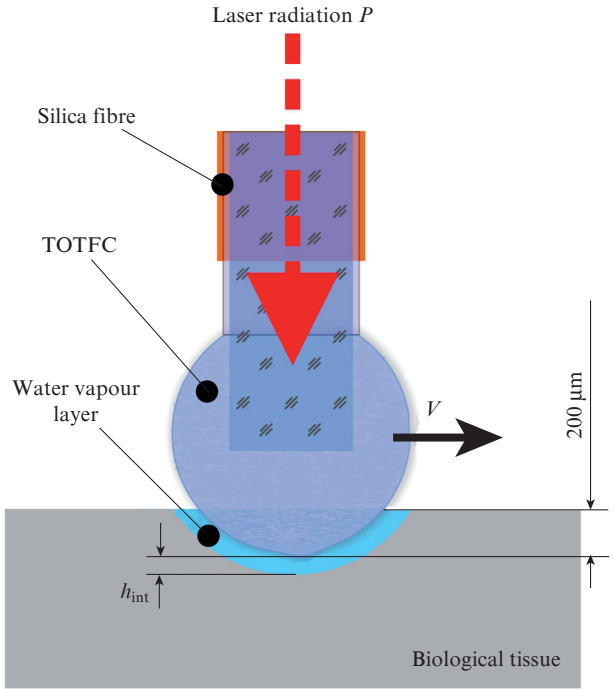

Figure 5. Scheme illustrating the interaction of the TOTFC with biological tissue.

Optical modelling was performed using the Monte Carlo method implemented in the programme TracePro®Expert-7.0.1 Release (Lambda Research Corporation, USA). Thermophysical modelling was performed in the COMSOL Multiphysics® software package (COMSOL Inc., USA; version No. 5.4).

Using the COMSOL Multiphysics® software package, the TOTFC geometric model was constructed identical to the structural one (see Section 2). This geometric model was part of the general geometric model, which, in addition to the TOTFC, also contains biological tissue and a layer of water vapour between them. In the COMSOL Multiphysics® software package, using the Heat Transfer in Solids and Time Dependent programmes of the general geometric model, the heat conduction equation was obtained in the form:

$$\rho c\frac{\partial T}{\partial t} = \frac{\partial}{\partial x}\left(\lambda\frac{\partial T}{\partial x}\right) + \frac{\partial}{\partial y}\left(\lambda\frac{\partial T}{\partial y}\right) + \frac{\partial}{\partial z}\left(\lambda\frac{\partial T}{\partial z}\right) + Q_w(x,y,z,t,T), \quad (1)$$

where ρ is the density; c is the specific heat; λ is the coefficient of thermal conductivity; and $Q_w(x,y,z,t,T)$ is the power of internal heat sources [characterises the power released by a heat source, located at a point with coordinates (x,y,z) at time t, with temperature T].

The above equation is the Fourier–Kirchhoff equation. It relates the temporal and spatial changes in temperature ∂T at any point in the body for a three-dimensional temperature field in a Cartesian coordinate system. To solve it, it is necessary to add uniqueness conditions, which include geometric, physical, initial and boundary conditions. In our case, the optical fibre with the TOTFC located on its distal end is placed vertically; the environment is air; there is no airflow; the initial temperature of the fibre, biological tissue, TOTFC and ambient air is the room temperature (here 300 K). In addition to natural convection, heat exchange with the environment was implemented via thermal radiation. For the input end of the optical fibre, the condition of thermal insulation was set. The conditions of heat exchange with the environment were specified by the Diffuse Surface programme.

In the COMSOL Multiphysics® software package, the solution to Eqn (1) is obtained by means of the finite difference method, using which a solid is represented as a set of nodes, i.e., the domain of continuous change of arguments (e.g., coordinate and time) is replaced by a finite (discrete) set of points called a grid. In addition to the geometric conditions, the knowledge of the numerical values of such thermophysical characteristics of the materials as density, specific heat, thermal conductivity and degree of blackness is also required for unambiguous solution to Eqn (1). The results of the analysis of a large number of reference information sources describing the temperature dependences of these thermophysical characteristics of the TOTFC are presented in Ref. [40]. In the present work, such an analysis allowed setting the temperature dependences of the thermophysical characteristics for biological tissue and water vapour (see below). In the COMSOL Multiphysics® software package, the calculation is programmed so that at each step such values of thermophysical characteristics are used that correspond to the temperature attained by the object (TOTFC, biological tissue, water vapour) by the end of the previous step.

It should be noted that the contribution of vapours produced by laser impact during laser processing of materials is widely discussed [44]. At the same time, because of the diversity and extreme complexity of the simultaneously occurring processes no complete adequate theoretical model of a gas-vapour channel has been created yet. The experimental data, however, indicate the mutual influence and competition of various physical processes and effects in the gas–vapour channel. In some cases, under the impact of laser radiation, the vapour is additionally heated, which increases the thermal load on the processed material. However, the use of the TOTFC has some specific features, namely, the converter itself efficiently absorbs radiation and the laser radiation practically does not penetrate into the resulting vapour layer, which makes it possible not to take into account the contribution of laser radiation to the formation of the vapour layer.

The fraction of laser radiation absorbed in the TOTFC corresponded to the value determined at the stage of optical modelling (see above), and the distribution of heat sources was uniform. Earlier in Ref. [40], attention was drawn to the fact that the thermophysical properties of the TOTFC can depend on temperature. These dependences were used in the calculations of the present study, too. In addition, the modelling took into account the effects of coagulation, dehydration and carbonisation of biological tissue.

Figure 6 shows the temperature dependences of density, specific heat, thermal conductivity coefficient, and degree of blackness for the soft biological tissue (chicken thigh muscle tissue) [45–56], and Fig. 7 shows similar parameters for water vapour [57–60].

The temperature dependences of the degree of blackness of the titanium-doped converter [40], biological tissue (Fig. 6d) and water vapour (Fig. 7d) made it possible to allow for the contribution of the secondary radiation from the burning-hot converter.

The temperature dependences of the biotissue–air and vapour–air heat transfer coefficients corresponded to those of the built-in library of COMSOL Multiphysics® (COMSOL Inc., USA; version number 5.4).

Within the framework of the proposed model, we determined the relationship between the thickness h_{int} of the water vapour layer, on the one hand, and the average power of laser radiation and the velocity of the TOTFC movement, on the other hand (Fig. 8). The layer thickness h_{int} was determined as a result of an iterative calculation, the purpose of which was

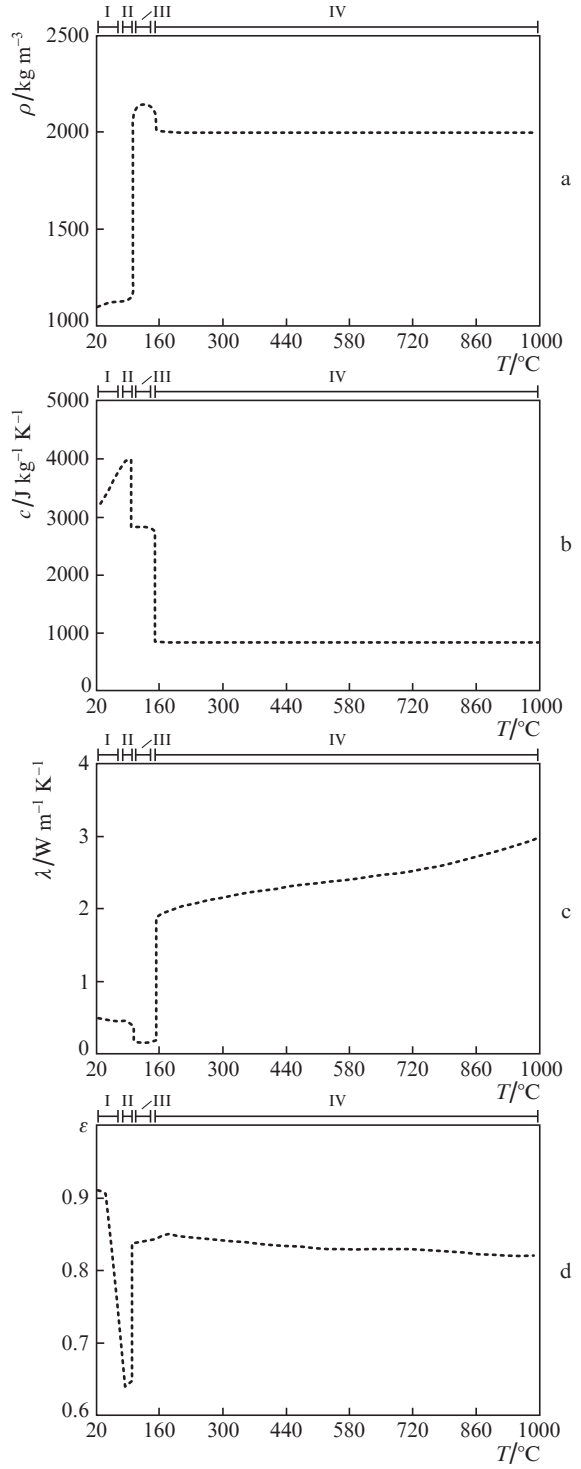

Figure 6. Dependences of (a) density, (b) specific heat, (c) thermal conductivity and (d) degree of blackness of soft biological tissue on temperature: (I) intact biotissue, (II) coagulated biotissue, (III) dehydrated biotissue, (IV) carbonised biotissue (amorphous carbon) [45–56].

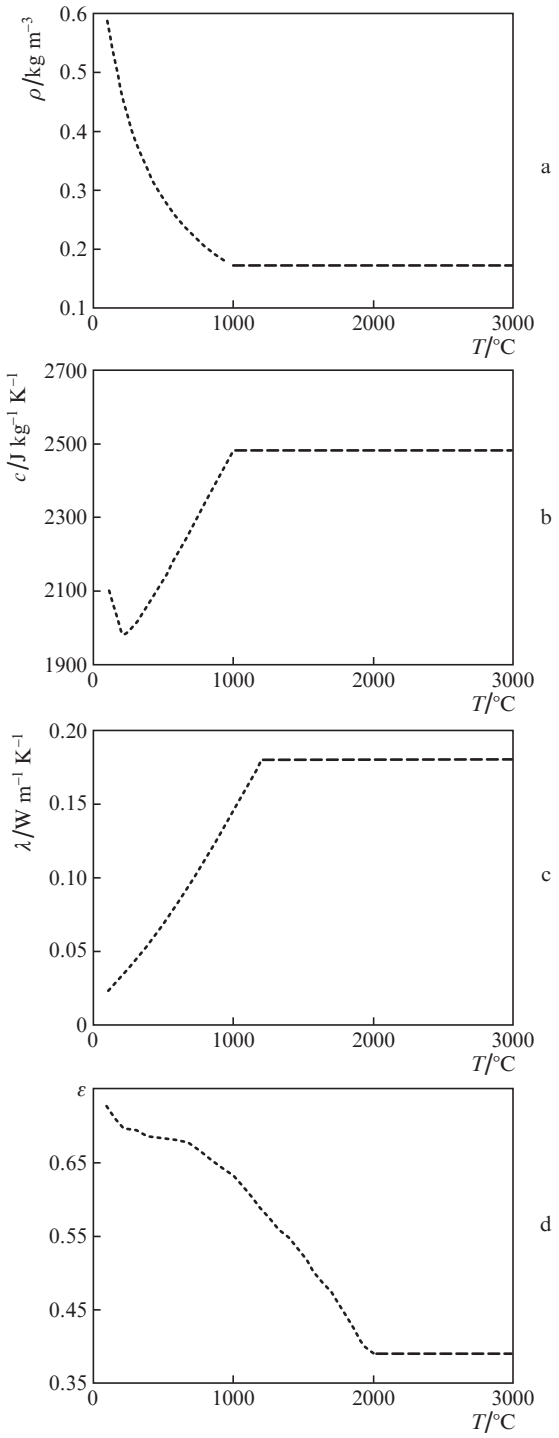

Figure 7. Dependences of (a) physical density, (b) specific heat, (c) thermal conductivity coefficient and (d) degree of blackness of water vapour as a function of temperature: the dotted curve shows the data [57–60], and the dashed line is the approximation.

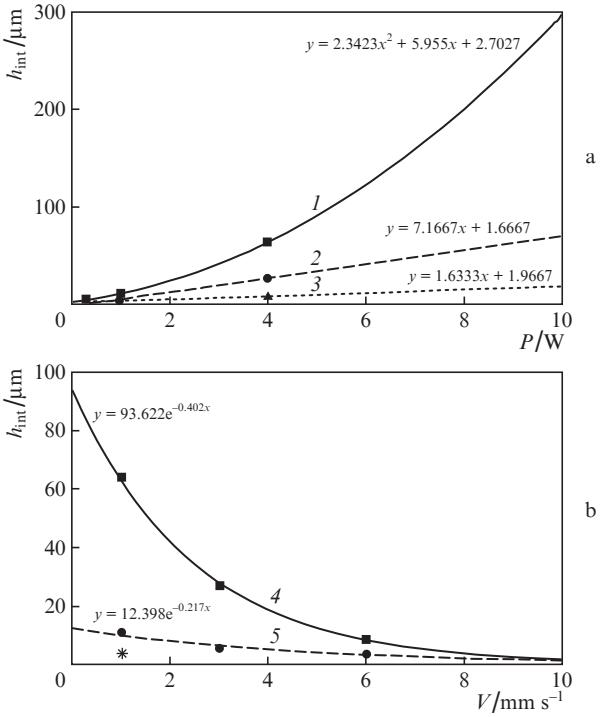

Figure 8. Dependences of the thickness h_{int} of the water vapour layer between the TOTFC and the biotissue on (a) the average laser radiation power and (b) the speed of the converter movement along the surface of the biotissue. Points are the results of iterative calculations, and curves are the approximations. Curves (*1*), (*2*), and (*3*) correspond to $V = 1, 3$, and 6 mm s^{-1}, and curves (*4*) and (*5*) correspond to $P = 4.0$ and 1.0 W; an asterisk corresponds to $P = 0.3$ W.

to achieve the coincidence of the values of the theoretical and experimental temperatures of the TOTFC averaged over the entire volume of the converter at a given average laser radiation power and the converter moving speed. Based on the results of the iterative calculation, approximation dependences of h_{int} on the average laser radiation power and the speed of converter movement were also plotted in Fig. 8. It is seen that with an increase in the average laser radiation power, the thickness of the water vapour layer between the converter and the biological tissue increases, and with an increase in the speed of the converter moving along the biological tissue surface h_{int} decreases. As a result of the modelling, the spatial distributions of temperature in the biological tissue were determined at various average powers of laser radiation with a wavelength of 980 nm and the speeds of the TOTFC movement along the surface of the biological tissue. The calculated results were compared with the experiment, and the boundaries of the carbonisation and coagulation zones of laser wounds were compared with the isotherms for temperatures characteristic of these effects.

The appearance of a laser wound formed in soft biological tissue by the TOTFC with the average laser power of 4.0 W and the movement speed 1 mm s^{-1} is presented in Fig. 9. The same figure shows the distribution of temperature (isotherms) over the surface of the biological tissue, obtained by thermophysical modelling, the layer thickness of water vapour being $h_{int} = 64$ μm.

Figure 10 presents an NBTC image of a longitudinal section of the laser wound formed in the soft biological tissue at $P = 4.0$ W using a TOTFC moving with the speed $V = 1$ mm s^{-1} and the depth distribution of temperature (isotherms) in the biological tissue obtained by thermophysical modelling at $h_{int} = 64$ μm.

It can be seen that the boundary between the intact and coagulated biological tissue both on the surface (Fig. 9) and in the depth (Fig. 10) of the biological tissue coincides with the +60 °C isotherm. The boundary between the coagulated and carbonised biological tissue both on the surface (Fig. 9) and in the depth (Fig. 10) of the biological tissue coincides with the +150 °C isotherm.

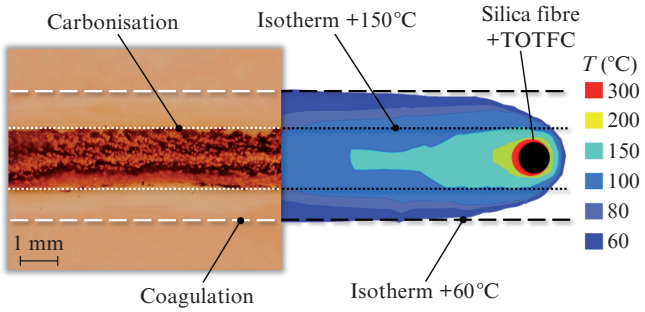

Figure 9. (Colour online) Photograph of the laser wound (left, [39]) and the temperature distribution on the surface of the biotissue obtained by modelling at $P = 4.0$ W and $V = 1$ mm s^{-1} ($h_{int} = 64$ μm).

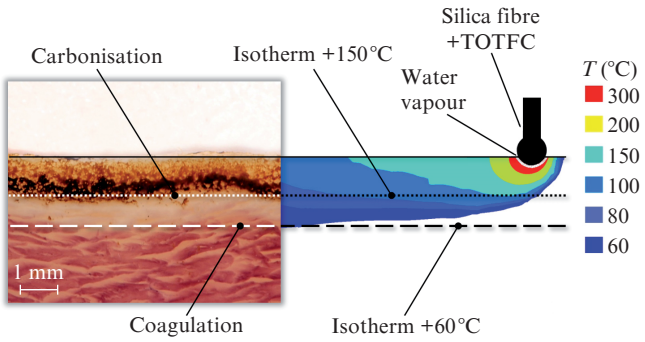

Figure 10. (Colour online) NBTC photograph of the laser wound longitudinal section (left, [39]) and the depth distribution of the biotissue temperature obtained by modelling at $P = 4.0$ W and $V = 1$ mm s^{-1} ($h_{int} = 64$ μm).

Coagulation and carbonisation of biological tissue result from the absorption of laser radiation by biological tissue with its subsequent heating and, in the general case, depend on the temperature and the time of exposure. During coagulation, the protein component of the biological tissue denatures and the tissue whitening is observed. During carbonisation, finely dispersed carbon is formed and the biological tissue is charred (blackens). The issues related to coagulation and carbonisation of biological tissue are thoroughly discussed in Refs [61–68]. For each biological tissue, the values of temperature and exposure time at which these effects are observed are individual, because in most cases, biological tissues are complex multicomponent media. Each component of biological tissue can be considered as a monostructure for which the temperature of thermal conversion (coagulation, carbonisation) can be determined experimentally and theoretically. For example, albumin can be considered such a monostructure, for which the relationship between the temperature and time

required for coagulation is determined [61], namely, albumin coagulation occurs during an exposure time of the order of one second at a temperature of 65 °C and in several hours at a temperature of 45 °C. At the same time, it is known that the denaturation rates for various protein structures can differ greatly from each other [62]. Thus, for native collagen fibres, fast denaturation occurs at a temperature of 80 °C [63]. In addition, the water content can strongly influence the coagulation temperature in a biological tissue. For example, cartilage during rapid heating does not denature even at a temperature close to 100 °C [63]. Thus, the temperature range in which coagulation is observed is very wide. In this regard, the calculated +60 °C isotherm coinciding with the visual boundary of the biological tissue whitening (Figs 9 and 10) can be considered an isotherm at which coagulation of the soft biological tissue occurs. The question of the carbonisation temperature of a biological tissue is not as clear as that of its coagulation temperature. In a number of publications, it is noted that in the range of 100–300 °C, the biotissue pyrolysis and burnout occur, and at a temperature of 150–200 °C, its carbonisation occurs. This is accompanied by the blackening of biological tissue and the appearance of smoke [64–66]. At a temperature of 250 °C, carbonisation of red blood cells occurs [67, 68]. It can be seen that, as in the case of coagulation, it is extremely difficult to indicate the generally accepted temperature at which carbonisation of biological tissue occurs, so only a certain temperature range can be determined. Obviously, this is due to a variety of factors affecting the value of the carbonisation temperature, including the composition of the biological tissue, the measurement technique, the environment, etc. In our case, the +150 °C isotherm coincides with the boundary of the biological tissue blackening (carbonisation), visually distinguishable in the experiment, and according to Refs. [65, 66], the temperature of 150 °C can correspond to the temperature of carbonisation occurrence.

Thus, the thermophysical model of the interaction of TOTFC with soft biological tissue, proposed in this work and implemented by means of the COMSOL Multiphysics® software package, taking into account the temperature dependence of the main thermophysical parameters of TOTFC and biological tissue, as well as the influence of the thickness of the water vapour layer between the converter and biological tissue, allows an adequate description of the effects observed in the experiment.

4. Conclusions

A new converter is considered, which allows significantly expanding the capabilities of contact laser surgery by reaching high temperatures in the field of interaction. High temperatures are attained due to the materials and structural features of the titanium-doped converter and earlier could be obtained only by changing the wavelength of the laser radiation. The temperature depends on the average power of the laser radiation and the speed of the TOTFC movement along the surface of the biological tissue. During excision of soft biological tissue, the temperature of the converter reaches 1980 ± 154 °C, while the ablation and coagulation depths of soft biological tissue are 1030 ± 150 and 720 ± 100 μm, respectively.

Structural, optical, and thermophysical models of the titanium-doped optothermal fibre converter of laser radiation are considered. In the experiment simulating the sequence of actions of a surgeon in laser contact surgery of soft tissue, we determined how the average laser radiation power and the speed of movement of the TOTFC along the surface of the tissue affect the converter temperature and the depth of tissue coagulation and ablation. For the first time, a model describing the interaction of the TOTFC with a soft biological tissue was proposed and compared with the experiment. This model takes into account the temperature dependences of the thermophysical parameters of the converter and biological tissue, as well as the contribution of the thickness of the layer of water vapour between the converter and the tissue. It is shown that the thickness of the water vapour layer has a significant effect on the temperature of the TOTFC.

Acknowledgements. This work was carried out as part of the Program of Increasing the Competitiveness of ITMO University Among the World Leading Research and Educational Centres for 2013–2020. (The '5 in 100' Programme, Grant 08-08).

References

1. Rai P.K., in *Emerging Trends in Laser & Spectroscopy and Applications* (New Delhi: Allied Publishers, 2010).
2. Romanos G., Nentwig G.H. *J. Clin. Laser Med. Surg.*, **17**, 193 (1999).
3. Sanz-Moliner J.D., Nart J., Cohen R.E., Ciancio S.G. *J. Periodontol.*, **84**, 152 (2013).
4. Romanos G.E., Belikov A.V., Skrypnik A.V., Feldchtein F.I., Smirnov M.Z., Altshuler G.B. *Laser. Surg. Med.*, **47**, 411 (2015).
5. Altshuler G.B. *Proc. 19th Annual Conf. of the Academy of Laser Dentistry* (Scottsdale, AZ, USA, 2012).
6. Jacques S.L. *Phys. Med. Biol.*, **58**, R37 (2013).
7. Kaufmann R., Hibst R. *Clin. Exp. Dermatol.*, **15**, 389 (1990).
8. Beer F., Körpert W., Passow H., Steidler A., Meinl A., Buchmair A.G., Moritz A. *Laser. Med. Sci.*, **27**, 917 (2012).
9. Capon A., Mordon S. *Am. J. Clin. Dermatol.*, **4** (1), 1 (2003).
10. Rizzo L.B., Ritchey J.W., Higbee R.G., Bartels K.E., Lucroy M.D. *J. Am. Vet. Med. Assoc.*, **225**, 1562 (2004).
11. Altshuler G.B., Belikov A.V., Skripnik A.V., Feldstein F.I. *Innovatsionnaya Stomatologiya*, **1**, 2 (2012).
12. Skripnik A.V. *Izv. Vyssh. Uchebn. Zaved., Ser. Priborostroenie*, **56**, 37 (2013).
13. Belikov A.V., Feldchtein F.I., Altshuler G.B. US Patent №2012/0123399 A1/ № 13/379,916; appl. 31.12.2010; pub. 17.05.2012.
14. Belikov A.V., Skrypnik A.V., Shatilova K.V. *Frontiers Optoelectron.*, **8**, 212 (2015).
15. Belikov A.V., Skripnik A.V., Kurnyshev V.Yu., Shatilova K.V. *Quantum Electron.*, **46** (6), 534 (2016) [*Kvantovaya Elektron.*, **46** (6), 534 (2016)].
16. Verdaasdonk R.M., Borst C., Boulanger L.H.M.A., van Gemert M.J.S. *Lasers Med. Sci.*, **2** (3), 153 (1987).
17. Berlien H.P., Müller G.J., in *Applied Laser Medicine* (Berlin: Springer-Verlag, 2003).
18. Abela G.S., in *Lasers in cardiovascular medicine and surgery: fundamentals and techniques* (Norwell: Kluwer Academic Publishers, 1990).
19. Belikov A.V., Gelfond M.L., Shatilova K.V., Semyashkina Y.V. *Proc. SPIE*, **9887**, 98871B-1 (2016).
20. Belikov A.V., Gelfond M.L., Shatilova K.V., Sosenkova S.A., Lazareva A.A., Semyashkina Y.V. *Proc. SPIE*, **9917**, 99170H-1 (2016).
21. Phillip C.M., Almohamad A., Adam M., Becker-Kohnlein J., Berlien H.P., Muller U., Poetke M., Urban P. *Photonics Lasers Med.*, **4** (3), 215 (2015).
22. Blokker R.S., Lock T.M.T.W., de Boorder T. *Laser. Surg. Med.*, **45** (9), 582 (2013).
23. Hennings D.R., Zaro M.A., Zimmerman E.M. US Patent 8439045 B2/ №13/631351; appl. 28.09.2012; pub. 14.05.2013.
24. Hennings D.R., Fullmer D.J. US Patent 8573227 B2/ №13/593467; appl. 23.08.2012; pub. 05.11.2013.
25. Giannelli M., Formigli L., Lasagni M., Bani D. *Photomed. Laser. Surg.*, **31** (5), 212 (2013).

26. Giannelli M., Formigli L., Bani D. *J. Periodontol.*, **85** (4), 554 (2014).
27. Üstün K., Erciyas K., Sezer U., Şenyurt S.Z., Gündoğar H., Üstün O., Öztuzcu S. *Photomed. Laser. Surg.*, **32** (2), 61 (2014).
28. Vandertop W.P., Verdaasdonk R.M., van Swol C.F.P. *J. Neurosurg.*, **88** (1), 82 (1998).
29. Willems P.W.A., Vandertop W.P., Verdaasdonk R.M., van Swol C.F.P., Jansen G.H. *Laser. Surg. Med.*, **28** (4), 24 (2001).
30. van Beijnum J., Hanlo P.W., Fischer K., Majidpour M.M., Kortekaas M.F., Verdaasdonk R.M., Vandertop W.P. *Neurosurgery*, **62** (2), 437 (2008).
31. Renner C., Frede T., Seemann O., Rassweiler J. *J. Endourol.*, **12** (6), 537 (1998).
32. Yelagin V.V., Shakhova M.A., Karabut M.M., Kuznetsova D.S., Bredikhin V.I., Prodanets N.N., Snopova L.B., Baskina O.S., Shakhov A.V., Kamenskiy V.A. *Sovremennye Tekhnologii v Meditsine*, **7** (3), 55 (2015).
33. Zhigar'kov V.S., Yusupov V.I., Tsypina S.I., Bagratashvili V.N. *Quantum Electron.*, **47** (10), 942 (2017) [*Kvantovaya Elektron.*, **47** (10), 942 (2017)].
34. Sapogova N., Bredikhin V., Bityurin N., Kamensky V., Zhigarcov V., Yusupov V. *Biomed. Opt. Express*, **8** (1), 104 (2017).
35. Kuznetsova D.S., Karabut M.M., Elagin V.V., Shakhova M.A., Bredikhin V.I., Baskina O.S., Snopova L.B., Shakhov A.V., Kamensky V.A. *Opt. Photonics J.*, **5** (1), 1 (2015).
36. Belikov A.V., Skrypnik A.V., Kurnyshev V.Y. *Proc. SPIE*, **9887**, 98873C-1 (2016).
37. Belikov A.V., Skripnik A.V. *Quantum Electron.*, **47** (7), 669 (2017) [*Kvantovaya Elektron.*, **47** (7), 669 (2017)].
38. *EPIC Pro: Re Inventing Diode Laser Soft Tissue Therapy Using Science* (Irvine, CA, USA: Biolase, Inc., 2016).
39. Belikov A.V., Skrypnik A.V. *Laser. Surg. Med.*, **51** (2), 185 (2019).
40. Belikov A.V., Skrypnik A.V., Salogubova I.S. *Proc. SPIE*, **11065**, 1106514-1 (2019).
41. Samsonov G.V. *The Oxide Handbook* (New York, Washington, London: IFI/Plenum, 1973).
42. Burachas S.F., Vasil'ev A.A., Ippolitov M.S., Man'ko V.I., Savel'ev Y.A., Tamulaitis G. *Crystallogr. Rep*+, **52** (6), 1088 (2007).
43. Kuhling H. *Handbuch der Physik* (Leipzig: Fachbuchverlag, 1962; Moscow: Mir, 1985).
44. Klimkov Yu.M., Mayorov V.S., Khoroshev M.V. *Vzaimodeistvie lazernogo izlucheniya s veshchestvom* (Interaction of Laser Radiation with Matter) (Moscow: MIIGAiK, 2014).
45. Murphy R.Y., Marks B.P. *J. Food Process Eng.*, **22**, 129 (1999).
46. Murphy R.Y., Marks B.P., Marcy J.A. *J. Food Sci.*, **63** (1), 88 (1998).
47. Delgado A.E., Sun D.W. *J. Food Eng.*, **55** (1), 1 (2002).
48. Chubik I.A., Maslov A.M. *Spravochnik po teplofizicheskim kharakteristikam pishchevykh produktov i polufabrikatov* (Handbook of Thermophysical Characteristics of Foodstuffs and Semi-Prepared Foods) (Moscow: Pishchevaya promyshlennost', 1970).
49. Rabia S., in *Thermal Properties of Foods* (New York City, U.S.: ASHRAE, 2006).
50. Sahin S., Sumnu S.G., in *Physical Properties of Foods. Food Science Text Series* (New York: Springer, 2006).
51. Henning K.-D., von Kienle H. *Carbon Ullmann's Encyclopedia of Industrial Chemistry*, **6**, 771 (2012).
52. Samsonov G.V. *Svoistva elementov* (Properties of Elements) (Moscow: Metallurgiya, 1976).
53. Ho C.Y., Powell R.P., Liley P.E. *J. Phys. Chem. Ref. Data*, **1** (2), 279 (1972).
54. Ibarra J.G., Tao Y., Cardarelli A.J., Shultz J. *Appl. Eng. Agric.*, **16** (2), 143 (2000).
55. Duck F. *Physical Properties of Tissue: A Comprehensive Reference Book* (San Diego: Academic Press, 1990).
56. Martynenko O.G. *Spravochnik po teploobmennikam* (Handbook of Heat Exchangers) (Moscow: Energoatomizdat, 1987).
57. Missenard A. *Conductivité thermique des solides, liquides, gaz et de leurs mélanges* (Paris: Éditions Eyrolles, 1965; Moscow: Mir, 1968).
58. Aleksandrov A.A., Grigor'ev B.A. *Tablitsy fizicheskikh svoistv vody i vodyanogo para* (Tables of Physical Properties of Water and Water Vapour) (Moscow: MEI, 1999).
59. Kazantsev Ye.I. *Promyshlennyye pechi* (Industrial Furnaces) (Moscow: Metallurgiya, 1975).
60. Acherkan N.S. *Spravochnik mashinostroitelya* (Handbook of a Mechanical Engineer) (Moscow: Mashgiz, 1956)].
61. Berlien H.-P., Muller G.J. *Applied Laser Medicine* (Berlin, Heidelberg, New York: Springer, 2003).
62. Huttman G., Birngruber R. *IEEE J. Sel. Top. Quantum Electron.*, **5** (4), 954 (1999).
63. Bagratashvili V.N., Baskov A.V., Borshchenko I.A., Ignat'yeva N.Yu., Ovchinnikov Yu.M., Omel'chenko A.I., Sviridov A.P., Svistushkin V.M., Sobol' E.N., Shekhter A.B. *Lazernaya inzheneriya khryashchei* (Laser Engineering of Cartilages) (Moscow: Fizmatlit, 2006).
64. Tuchin V.V. *Lazery i volokonnaya optika v biomeditsinskikh issledovaniyakh* (Lasers and Fibre Optics in Biomedical Research) (Moscow: Fizmatlit, 2010)].
65. Niemz M.H. *Laser Tissue Interactions: Fundamentals And Applications* (Berlin, Heidelberg, New York: Springer, 2007).
66. Eichier J., Seiler T. *Lasertechnik in der Medizin* (Berlin, Heidelberg, New York, London, Paris, Tokyo, Hong Kong, Barcelona, Budapest: Springer, 1991).
67. Kovalenko A.A., Minaev V.P. *Radiooptika. MGTU im. N.E. Baumana*, **5**, 101 (2015).
68. Minaev V.P. *Lazernye meditsinskie sistemy i meditsinskie tekhnologii na ikh osnove* (Laser Medical Systems and Medical Technologies Based on Them) (Dolgoprudnyi: Intellect, 2017).